

Limits on the gravity wave contribution to microwave anisotropies

J. P. Zibin and Douglas Scott

*Department of Physics and Astronomy, University of British Columbia, 6224 Agricultural Road,
Vancouver, BC V6T 1Z1 Canada*

Martin White

*Departments of Astronomy and Physics, University of Illinois at Urbana-Champaign, 1110 West
Green Street, Urbana, IL 61801-3080*

Abstract

We present limits on the fraction of large angle microwave anisotropies which could come from tensor perturbations. We use the *COBE* results as well as smaller scale CMB observations, measurements of galaxy correlations, abundances of galaxy clusters, and Ly α absorption cloud statistics. Our aim is to provide conservative limits on the tensor-to-scalar ratio for standard inflationary models. For power-law inflation, for example, we find $T/S < 0.52$ at 95% confidence, with a similar constraint for ϕ^p potentials. However, for models with tensor amplitude unrelated to the scalar spectral index it is still currently possible to have $T/S > 1$.

PACS numbers: 98.80.-k, 98.70.Vc.

I. INTRODUCTION

The presence of a primordial gravitational wave perturbation spectrum was an early prediction of inflationary models of the big bang [1]. However, it was not until the results of the *COBE* satellite mission that it became possible to begin to meaningfully constrain the tensor contribution to the overall perturbation spectrum [2–6]. In an early result, Salopek [6] found that, assuming power-law inflation, tensors must contribute less than about 50% of the cosmic microwave background (CMB) fluctuations at the 10° scale.

Since that time, ground- and balloon-based experiments have begun to fill in the smaller-scale regions of the CMB power spectrum. These scales are crucial for constraining the gravity wave contribution because the tensor spectrum is expected to be negligible on scales finer than $\sim 1^\circ$, and therefore large-scale power greater than that expected for scalars can be attributed to tensors. Markevich and Starobinsky [7] have set some stringent limits on the tensor contribution. For example, they found that the ratio of tensor to scalar components of the CMB spectrum is $T/S < 0.7$ at 97.5% confidence for a flat, cosmological-constant-free universe with $H_0 = 50 \text{ kms}^{-1}\text{Mpc}^{-1}$. However, their analysis used a limited CMB data set and considered only a restricted set of values for the cosmological parameters. Recently Tegmark [8] has performed an analysis using a compilation of CMB data, and found a 68% upper confidence limit of 0.56 on the tensor to scalar ratio. In this work specific inflationary models were not considered, but a number of parameters were allowed to vary freely. In another recent study Lesgourgues *et al.* [9] analysed a particular broken-scale-invariance model of inflation with a steplike primordial perturbation spectrum, and found that the tensor to scalar ratio can reach unity. Melchiorri *et al.* [10] placed limits on tensors allowing for a blue scalar spectral index, and indeed found that blue spectra and a large tensor component are most consistent with CMB observations.

Our aim here is to provide a more comprehensive answer (or set of answers) to the question: how big can T/S be? We present constraints on tensors for specific models of inflation as well as for freely varying parameters. In all cases we marginalize over the important, but as yet undetermined, cosmological parameters. We use both *COBE* and small-scale CMB data, as well as information about the matter power spectrum from galaxy correlation, cluster abundance, and Lyman α forest measurements. We refer to these various measurements of the power spectra as “data sets”. We additionally consider the effect, for each data set, of various observational constraints on the cosmological parameters, such as the age of the universe, cluster baryon density, and recent supernova measurements. We refer to these constraints as “parameter constraints” (this separation between “data sets” and “parameter constraints” is somewhat subjective, but dealt with consistently in our Bayesian approach; it is conceptually simpler to consider power spectrum constraints as measurements with some Gaussian error, while regarding allowed limits on cosmological parameters as restrictions on parameter space). Finally we consider what implications our results have for the direct detection of primordial gravity waves.

II. INFLATION MODELS

Our goal is to provide limits on the tensor contribution to the primordial perturbation spectra using a variety of recent observations. In models of inflation, the scalar (density) and tensor (gravity wave) metric perturbations produced during inflation are specified by two spectral functions, $A_S(k)$ and $A_T(k)$, for wave number k . These spectra are determined by the inflaton potential $V(\phi)$ and its derivatives [11]. However, when comparing model predictions with actual observations of the CMB, it is more useful to translate the inflationary spectra into the predicted multipole expansions of the CMB temperature field: $\Delta T/T(\theta, \phi) = \sum_{\ell m} a_{\ell m} Y_{\ell m}(\theta, \phi)$, where $Y_{\ell m}(\theta, \phi)$ are the spherical harmonics. The spectrum $C_\ell \equiv \langle |a_{\ell m}|^2 \rangle$ can be decomposed into scalar and tensor parts, $C_\ell = C_\ell^S + C_\ell^T$. In the literature the tensor to scalar ratio is conventionally specified either at $\ell = 2$ or in the spectral plateau at $\ell \simeq 10 - 20$. Here we have chosen the $\ell = 2$ or quadrupole moments of the temperature field, and write $S \equiv 5C_2^S/4\pi$ and $T \equiv 5C_2^T/4\pi$ as usual [12].

In order to constrain the tensor contribution T/S , we need to specify the particular model of inflation under consideration. This is because the model may provide a specific relationship between the ratio T/S and the scalar spectral index n_s . Except in Sec. VI we only consider spatially flat inflation models (*i.e.* $\Omega_0 + \Omega_\Lambda = 1$, where Ω_0 and $\Omega_\Lambda = \Lambda/(3H_0^2)$ are the fractions of critical density due to matter and a cosmological constant, respectively). In addition, we do not consider the “quintessence” models [13,14], where a significant fraction of the critical density is currently in the form of a scalar field with equation-of-state different from that of matter, radiation, or cosmological constant (although it would not be difficult to extend our results for explicit models with recent epoch dynamical fields). We will also restrict ourselves to models which use the slow-roll approximation, and incorporate only a single *dynamical* field – a class of models sometimes called “chaotic inflation” [15]. This is not as restrictive as it might sound, since most viable inflationary models are of this form. Although some genuinely two-field models are known [16], many multi-field models, the “hybrid” class, have only one field dynamically important and in these cases we effectively regain the single field case [17,18]. In addition, theories which modify general relativity (*e.g.* “extended” inflation [19,20]) can often be recast as ordinary general relativity with a single effective scalar field [21,18].

It is convenient to classify inflationary models as either “small-field”, “large-field”, or the already mentioned hybrid models [22]. Small-field models are characterized by an inflaton field which rolls from a potential maximum towards a minimum at $\langle \phi \rangle \neq 0$. These models generally produce negligible tensor contribution, but may result in the spectral index n_s differing significantly from scale invariance [11]. In hybrid models, the important scalar field rolls towards a potential minimum with non-zero vacuum energy. These models also typically have very small T/S , and the scalar index can be greater than unity [11]. The large-field models involve so-called “chaotic” initial conditions, where an inflaton initially displaced from the potential minimum rolls towards the origin. Large-field models can produce large T/S and $1 - n_s$, and these are the models considered in this paper. This is not to say that small-field and hybrid models are not interesting; on the contrary, current views of inflation in the particle physics context suggest that T/S is expected to be small [23]. However, large-field models must be considered when examining the observational evidence for a large tensor contribution.

It is also worth pointing out that we could construct models with a dip in the scalar power spectrum at large scales which compensates for the tensor contribution. Although we have not explored detailed models, we imagine that in principle models could be constructed with arbitrarily high T/S . We consider all such models with features at relevant scales to be unappealing unless there are separate physical arguments for them.

In addition to considering models with free scalar index and tensor contribution T/S , we shall thus focus on two classes of inflationary models which can be considered representative of those predicting large gravity wave contributions. Both are restricted to “red” spectral tilts, $n_S \leq 1$. The first, “power-law inflation” (PLI) [24,25], is characterized by exponential inflaton potentials of the form

$$V(\phi) \propto \exp \sqrt{\frac{16\pi\phi^2}{qm_{\text{Pl}}^2}}, \quad (1)$$

and results in a scale factor growth $a(t) \propto t^q$, hence the name. For PLI the tensor-to-scalar ratio in k -space can be calculated exactly as a function of n_S :

$$\frac{A_{\text{T}}^2(k)}{A_{\text{S}}^2(k)} = \frac{1 - n_S}{3 - n_S}. \quad (2)$$

Note the tensor contribution is directly related to the scalar spectral index n_S , which is further related to the tensor spectral index $n_{\text{T}} = n_S - 1$ in this model. Converting from k -space to the observed anisotropy spectrum introduces a dependence on the cosmological constant which can be approximated by [12]

$$T/S = -7\tilde{n} \left[0.97 + 0.58\tilde{n} + 0.25\Omega_{\Lambda} - \left(1 + 1.1\tilde{n} + 0.28\tilde{n}^2 \right) \Omega_{\Lambda}^2 \right], \quad (3)$$

where $\tilde{n} \equiv n_S - 1 = n_{\text{T}}$. The dependence on Λ arises because of different evolution for scalars and tensors when Λ dominates at late times. The dependence on other cosmological parameters is negligible [12].

We also consider the large-field polynomial potentials,

$$V(\phi) \propto \phi^p, \quad (4)$$

for integral $p > 1$ [26]. In this case both n_S and n_{T} are determined by the exponent p [11]:

$$n_S = 1 - \frac{2p + 4}{p + 200}, \quad (5)$$

$$n_{\text{T}} = \frac{-2p}{p + 200}. \quad (6)$$

The tensor index may be related to T/S through the consistency relation [12]

$$\frac{T}{S} = -7 \frac{f_{\text{T}}^{(0)}}{f_{\text{S}}^{(0)}} n_{\text{T}}, \quad (7)$$

where the cosmological parameter dependence, again dominated by Ω_Λ , can be approximated by

$$f_S^{(0)} = 1.04 - 0.82\Omega_\Lambda + 2\Omega_\Lambda^2, \quad (8)$$

$$f_T^{(0)} = 1.0 - 0.03\Omega_\Lambda - 0.1\Omega_\Lambda^2. \quad (9)$$

As a third possibility, we will also consider models with scalar index varying over the range $n_S = 0.8 - 1.2$, but with an independently varying tensor contribution T/S .

III. MICROWAVE BACKGROUND ANISOTROPIES

In order to evaluate likelihoods and confidence limits for T/S based on CMB measurements, we performed χ^2 fits of model C_ℓ spectra to CMB data. We did this for a set of “band-power” estimates of anisotropy at different scales, and separately for the *COBE* data themselves. For our first approach, we used a collection of binned data to represent the anisotropies as a function of ℓ . Specifically we took the flat-spectrum effective quadrupole values listed in Smoot and Scott [27] and binned them into nine intervals separated logarithmically in ℓ . We chose this simplified approach since we anticipated a large computational effort in covering a reasonably large parameter space. The use of binned data has been shown elsewhere [28] to give similar results to more thorough methods. If anything, there is a bias towards lowering the height of any acoustic peak, inherent in the simplifying assumption of symmetric Gaussian error bars [29]; for placing upper limits on T/S our approach is therefore conservative. We are also erring on the side of caution by using the binned data only up to the first acoustic peak, neglecting constraints from detections and upper limits at smaller angular scales.

We ignored the effect of reionization on the C_ℓ spectra. Reionization to optical depth τ reduces the power of small-scale anisotropies by $e^{-2\tau}$. Thus, in placing upper limits on T/S , it is conservative to set $\tau = 0$.

A fitting function for the spectrum, valid up to the first peak at $l \simeq 220$, has been provided by White [30]:

$$C_l(\nu) = \left(\frac{l}{10}\right)^\nu C_l(\nu = 0), \quad (10)$$

where ν is the (nearly) degenerate combination of cosmological parameters

$$\nu \equiv n_S - 1 - 0.32 \ln(1 + 0.76r) + 6.8(\Omega_B h^2 - 0.0125) - 0.37 \ln(2h) - 0.16 \ln(\Omega_0). \quad (11)$$

Here $r \equiv 1.4C_{10}^T/C_{10}^S$ is the tensor to scalar ratio at $\ell = 10$, normalized to provide $r = T/S$ for $\Omega_0 = 1$ and $n_S \rightarrow 1$. The parameter h is defined through $H_0 = 100h \text{ km s}^{-1} \text{ Mpc}^{-1}$, and Ω_B is the fraction of the critical density in baryons. Thus the standard CDM (sCDM) spectrum is specified by $\nu = 0$. We found that the Ω_Λ dependence of r can be well captured by introducing the rescaled variable r' , defined by

$$r' = \frac{r}{0.94 + 1.105\Omega_\Lambda^{3.75}}, \quad (12)$$

and setting $r' \equiv T/S$.

We fitted the model spectra of Eq. (10) to the binned data as follows. For each combination of parameters $(h, \Omega_B h^2, \Omega_0, n_S, T/S)$ we normalized the model spectrum to the binned data, and evaluated the likelihood $\mathcal{L}(h, \Omega_B h^2, \Omega_0, n_S, T/S) \propto \exp(-\chi^2/2)$. Next this likelihood was integrated, uniformly in the parameter, over the ranges of $h = 0.5 - 0.8$, $\Omega_B h^2 = 0.007 - 0.024$, and $\Omega_0 = 0.25 - 1$, subject to the constraints of Eq. (3) for PLI and Eqs. (5), (6), and (7) for polynomial potentials. For the case of free T/S , the scalar index was varied in the range $n_S = 0.8 - 1.2$. Finally the resultant $\mathcal{L}(T/S)$ was normalized to a peak value of unity and the 95% confidence limits evaluated. We tried to choose reasonable ranges for the prior probability distributions of the “nuisance parameters”, guided by the current weight of evidence. We checked that mild departures from our adopted ranges lead to only small modifications to our results. However, we caution that our conclusions will not necessarily be applicable for models which lie significantly outside the parameter space we considered. In addition, note that according to Eq. (11) we can crudely estimate an upper limit on T/S by combining the observational lower limit on ν with the maximal baryon density and minimal Ω_0 and h from our parameter ranges. However, this turns out to be an overly conservative estimate: for example, for $n_S = 1$, and using a lower limit of $\nu = -0.2$, Eq. (11) gives an upper limit of $T/S = 3.8$, compared with the limit $T/S = 1.6$ from Sec. VII.

For the separate constraint from the *COBE* data, we used the software package CMB-FAST [31] to calculate likelihoods based only on the *COBE* results at large scales. CMB-FAST calculates the spectrum using a line-of-sight integration technique. It then calculates likelihoods by finding a quadratic approximation to the large scale spectrum and using the *COBE* fits of Bunn and White [32]. These likelihoods were integrated and 95% limits calculated as above, except that the baryon density was fixed at $\Omega_B = 0.05$ to save computation time (and since Ω_B has negligible affect at these scales). The results of this procedure are presented in Sec. VII.

IV. LARGE-SCALE STRUCTURE

A. Galaxy correlations

We next applied observations of galaxy correlations to constrain T/S indirectly through the power spectrum of the density fluctuations, $\Delta^2(k)$. The power spectrum $\Delta^2(k)$ is expressed, following Bunn and White [32], by

$$\Delta^2(k) = \delta_H^2 \left(\frac{ck}{H_0} \right)^{3+n_S} T^2(k). \quad (13)$$

Here δ_H is the (Ω_0 , n_S , and r dependent) normalization described in Sec. IV B, and $T(k)$ is the transfer function which describes the evolution of the spectrum from its primordial form to the present.

We explicitly used for the transfer function the fit of Bardeen *et al.* [33],

$$T(q) = \frac{\ln(1 + 2.34q)}{2.34q} \left[1 + 3.89q + (16.1q)^2 + (5.46q)^3 + (6.71q)^4 \right]^{-1/4}, \quad (14)$$

with the scaling of Sugiyama [34]

$$q = \frac{k(T_{\gamma 0}/2.7 \text{ K})^2}{\Omega_0 h^2 \exp\left(-\Omega_B - \sqrt{h/0.5} \Omega_B/\Omega_0\right)}. \quad (15)$$

Here $T_{\gamma 0}$ is the temperature of the CMB radiation today.

We performed χ^2 fits of the (unnormalized) model power spectrum given by Eqs. (13) - (15) to the compilation of data provided in Table I of Peacock and Dodds [35], excluding their four smallest scale data points. These points were omitted because, while there are theoretical reasons [36] to expect that the galaxy bias approaches a constant on large scales, at the smallest scales the assumption of a linear bias appears to break down [37]. Here we are fitting for the *shape* of the matter power spectrum, ignoring the overall amplitude, since the normalization is complicated by the ambiguities of galaxy biasing.

The fitting was performed in exactly the same way as was described in Sec. III for the binned microwave anisotropies. Namely the model curves were normalized to the Peacock and Dodds data, the integrated likelihood was calculated, and the 95% confidence limits for n_S were evaluated. Since the shape of the power spectrum [Eq. (15)] is independent of the tensor amplitude, this technique can only provide limits on T/S when T/S is determined by the spectral index. That is, the galaxy correlation data can only constrain T/S for our PLI and ϕ^p cases, using the relationships [Eq. (3) or Eqs. (5), (6), and (7)] between T/S and n_S .

B. Cluster abundance

A very useful quantity for constraining the *amplitude* of the power spectrum is the dispersion of the density field smoothed on a scale R , defined by

$$\sigma^2(R) = \int_0^\infty W^2(kR) \Delta^2(k) \frac{dk}{k}. \quad (16)$$

Here $W(kR)$ is the smoothing function, which we take to be a spherical top-hat specified by

$$W(kR) = 3 \left[\frac{\sin(kR)}{(kR)^3} - \frac{\cos(kR)}{(kR)^2} \right]. \quad (17)$$

Traditionally the dispersion is quoted at the scale $8h^{-1}$ Mpc, and given the symbol σ_8 . For our experimental value we used the result of Viana and Liddle [38], who analysed the abundance of large galaxy clusters to obtain

$$\sigma_8 = 0.56 \Omega_0^{-0.47}, \quad (18)$$

with relative 95% confidence limits of $-18 \Omega_0^{0.2 \log_{10} \Omega_0}$ and $+20 \Omega_0^{0.2 \log_{10} \Omega_0}$ percent. Several other estimates have been published; the one we used is fairly representative, and with a more conservative error bar than most.

To compare this experimental result with the model value predicted by Eq. (16), we must fix the normalization δ_H . We used the result of Liddle *et al.* [39] who fitted δ_H using the *COBE* large scale normalization to obtain

$$10^5 \delta_{\text{H}}(n_{\text{S}}, \Omega_0) = 1.94 \Omega_0^{-0.785-0.05 \ln \Omega_0} \exp[f(n_{\text{S}})], \quad (19)$$

where

$$f(n_{\text{S}}) = \begin{cases} -0.95\tilde{n} - 0.169\tilde{n}^2, & \text{No tensors,} \\ 1.00\tilde{n} + 1.97\tilde{n}^2, & \text{PLI.} \end{cases} \quad (20)$$

For the case of non-PLI tensors, we used the fitting form of Bunn *et al.* [40]:

$$10^5 \delta_{\text{H}} = 1.91 \Omega_0^{-0.80-0.05 \ln \Omega_0} \frac{\exp(-1.01\tilde{n})}{\sqrt{1 + (0.75 - 0.13\Omega_{\Lambda}^2) r}} (1 + 0.18\tilde{n}\Omega_{\Lambda} - 0.03r\Omega_{\Lambda}). \quad (21)$$

We calculated likelihoods for our model σ_8 using a Gaussian with peak and 95% limits specified by Eq. (18), and then integrated \mathcal{L} and found limits for T/S as in the binned microwave case.

C. Lyman α absorption cloud statistics

Another measure of the amplitude of the matter power spectrum has been obtained recently by Croft *et al.* [41], who analysed the Lyman α (Ly α) absorption forest in the spectra of quasars at redshifts $z \simeq 2.5$. These results apply at smaller comoving scales than the cluster abundance σ_8 measurements, and hence are potentially more constraining. Croft *et al.* found

$$\Delta^2(k_p) = 0.57_{-0.18}^{+0.26} \quad (22)$$

at 1σ confidence, where the effective wavenumber $k_p = 0.008(\text{km s}^{-1})^{-1}$ at $z = 2.5$.

These results cannot be directly compared with the model predictions of Eq. (13), because Eq. (13) provides its predictions for the current time, *i.e.* $z = 0$. To translate to $z = 2.5$, we must first convert the model k from the comoving Mpc^{-1} units conventionally used in discussions of the matter power spectrum to $(\text{km s}^{-1})^{-1}$ at $z = 2.5$, using

$$k[(\text{km s}^{-1})^{-1}] = \frac{1+z}{H(z)} k[\text{Mpc}^{-1}], \quad (23)$$

where

$$H(z) = H_0 \sqrt{\Omega_0(1+z)^3 + \Omega_{\Lambda}} \quad (24)$$

for flat universes.

Next, we must consider the growth of the perturbations themselves. In a critical density universe (and assuming linear theory), the growth law is simply $\Delta^2(k, z) = \Delta^2(k, 0)(1+z)^{-2}$. As Ω_{Λ} increases, the growth is suppressed, and this can be accounted for by writing

$$\Delta^2(k, z) = \Delta^2(k, 0) \frac{g^2[\Omega(z)]}{g^2(\Omega_0)} \frac{1}{(1+z)^2}, \quad (25)$$

where the growth suppression factor $g(\Omega)$ can be accurately parametrized by [42]

$$g(\Omega) = \frac{5}{2}\Omega \left(\frac{1}{70} + \frac{209\Omega}{140} - \frac{\Omega^2}{140} + \Omega^{4/7} \right)^{-1}, \quad (26)$$

and the redshift dependence of Ω is given by

$$\Omega(z) = \Omega_0 \frac{(1+z)^3}{1 - \Omega_0 + (1+z)^3\Omega_0}, \quad (27)$$

all for spatially flat universes.

We calculated likelihoods using the normalized model predictions of Eq. (13), translated to $z = 2.5$ as described above, and then obtained limits for T/S as in the cluster abundance case.

V. PARAMETER CONSTRAINTS

A. Age of the universe

In flat Λ models, the age of the universe is [42]

$$t_0 = \frac{2}{3H_0} \frac{\sinh^{-1} \left(\sqrt{\Omega_\Lambda/\Omega_0} \right)}{\sqrt{\Omega_\Lambda}}. \quad (28)$$

During the integration of the likelihoods, we investigated the effect of imposing a constraint on the parameters h and Ω_0 , so that regions of parameter space corresponding to ages below various limits were excluded. This simply corresponds to a more complex form for the priors on the parameters. The precise limit on the age of the universe is a matter of on-going debate (*e.g.* [43,44]). A lower limit of around 11 Gyr now seems to be the norm, so we considered this case explicitly. We also considered the effect of a more constraining limit of 13 Gyr, still preferred by some authors.

B. Baryons in clusters

Recent measurements of the baryon density in clusters have suggested low Ω_0 for consistency with nucleosynthesis. We chose to use the results of White and Fabian [45] for the baryon density

$$\frac{\Omega_B}{\Omega_0} = (0.056 \pm 0.014)h^{-3/2}, \quad (29)$$

where the errors are at the 1σ level. We explored the implications of applying this constraint during the likelihood integrations, by adding a term

$$\left(\frac{h^{3/2}\Omega_B/\Omega_0 - 0.056}{0.014} \right)^2 \quad (30)$$

to each value of χ^2 .

C. Supernova constraints

Measurements of high- z Type-Ia supernovae (SNe Ia) are in principle well-suited to constraining Ω_0 on the assumption of a flat Λ universe, since such measurements are sensitive to (roughly) the difference between Ω_0 and Ω_Λ . We used the experimental results of Filippenko and Riess of the High- z Supernova Search team [46], who found for flat Λ models

$$\Omega_0 = 0.25 \pm 0.15 \quad (31)$$

at 1σ confidence. We also investigated the effect of applying this constraint as above.

VI. OPEN MODELS

For models with open geometry the situation is more complicated, and so we restrict ourselves to a brief discussion here. In addition to the added technical complexity involved in working in hyperbolic spaces, the presence of an additional scale, the curvature scale, renders ambiguous the meaning of scale-invariant fluctuations. For the most obvious scale-invariant spectrum of gravity wave modes, the quadrupole anisotropy actually diverges! For this reason one requires a definite calculation of the fluctuation spectrum from a well realized open model. The advent of open inflationary models [47] has allowed, for the first time, a *calculation* of the spectrum of primordial fluctuations in an open universe. As with all inflationary models, a nearly scale-invariant spectrum of gravitational waves (tensor modes) is produced [48,49]. The size of these modes in k -space, and their relation to the spectral index, is not dissimilar to the flat space models we have been considering. In the inflationary open universe models the spectrum of perturbations is cut-off at large spatial scales, leading to a finite gravity wave spectrum. However, the exact scale of the cutoff depends on details of the model, introducing further model dependence into the ℓ -space predictions.

Since gravitational waves provide anisotropies but no density fluctuations, their presence will in general lower the normalization of the matter power spectrum (for a fixed large angle CMB normalization). Open models already have quite a low normalization [50,51], so the most conservative limits on gravity waves come from models which produce the *minimal* tensor anisotropies, i.e. where the cutoff operates as efficiently as possible. The *COBE* normalization for such models with PLI is [52]

$$10^5 \delta_H = 1.95 \Omega_0^{-0.35-0.19 \ln \Omega_0 + 0.15 \tilde{n}} \exp(1.02 \tilde{n} + 1.70 \tilde{n}^2) . \quad (32)$$

Combining this normalization with the cluster abundance gives a strong constraint on T/S . We show in Fig. 1 the 95% CL upper limit on T/S as a function of Ω_0 in these models.

VII. RESULTS

Figure 2 presents likelihoods, integrated over the parameter ranges described above, and plotted versus T/S , for the various data sets, and specifically for PLI models. For the curve labelled “combined”, likelihoods for each data set (except the *COBE* data) were multiplied

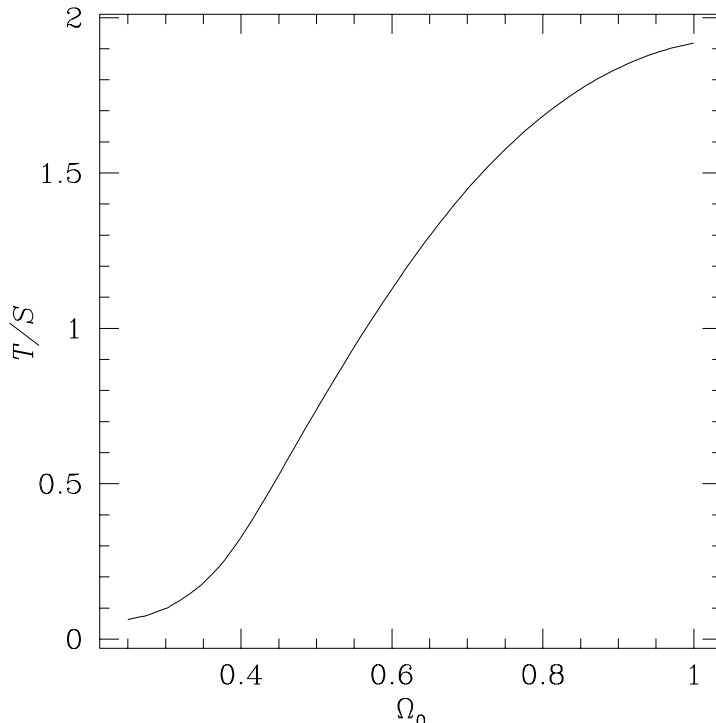


FIG. 1. 95% upper confidence limits on T/S for the open models described in the text. The cluster abundance data set was used with no parameter constraints.

together before integration. (Including the *COBE* data would have been redundant, since the binned CMB set already contains the *COBE* results.) Thus the “combined” values represent joint likelihoods for the relevant data sets, on the assumption of independent data. Note that the combined data curve of Fig. 2 differs significantly from the product of the already marginalized curves for the different data sets, which indicates that parameter covariance is important here. Also, the maximum joint likelihood in Fig. 2 corresponds to $\chi^2 \simeq 9$, which indicates a good fit for the 15 degrees of freedom involved.

Figure 3 displays integrated likelihoods versus T/S for each data set and for the combined data, again on the assumption of PLI. The effect of each parameter constraint is illustrated. The *COBE* data shape constraint is very weak, and exhibits essentially no cosmological parameter dependence, as expected. Thus the parameter constraints have little effect on the likelihoods, and the curves are not shown here. Cluster abundance is not much more constraining than the *COBE* shape, but exhibits considerably stronger cosmological parameter dependence, and hence is affected substantially by the various parameter constraints. The matter power spectrum shape constraint is so weak that we do not plot it here. The strongest constraint comes from the binned CMB data, and indeed these data dominate the joint results.

We can understand the general features of the large parameter dependence exhibited by the likelihoods for the matter spectrum data sets as follows. Near Λ CDM parameter values, it is well known that the matter power spectrum contains too much small-scale power when *COBE*-normalized at large scales. The presence of tensors improves the fit at small scales by decreasing the *scalar* normalization at *COBE* scales. Reducing h or Ω_0 , however, also

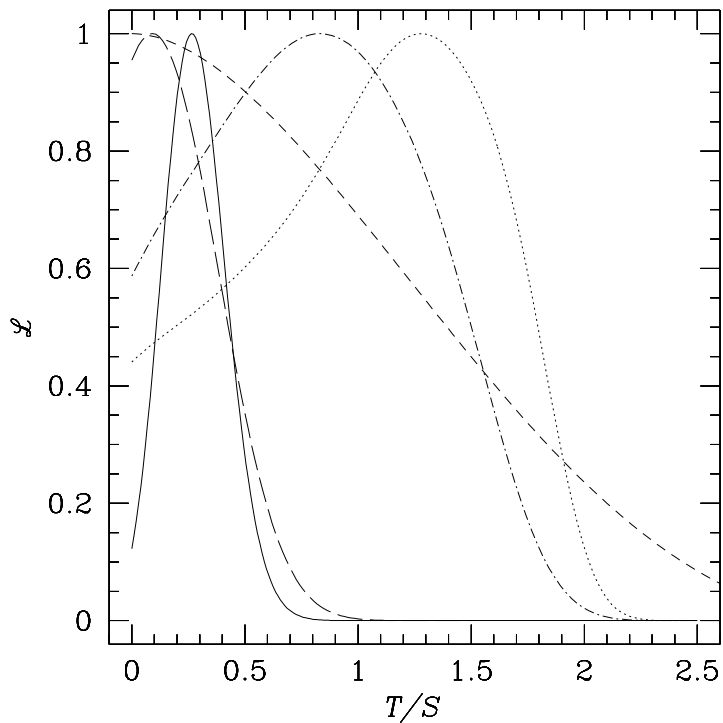


FIG. 2. Integrated likelihoods versus T/S for the various data sets: short-dashed, long-dashed, dotted, dash-dotted, and solid curves represent respectively *COBE*, binned CMB, cluster abundance, $\text{Ly}\alpha$ absorption, and combined data. All curves are for PLI inflation, using the priors discussed in Sec. III, with no additional parameter constraints.

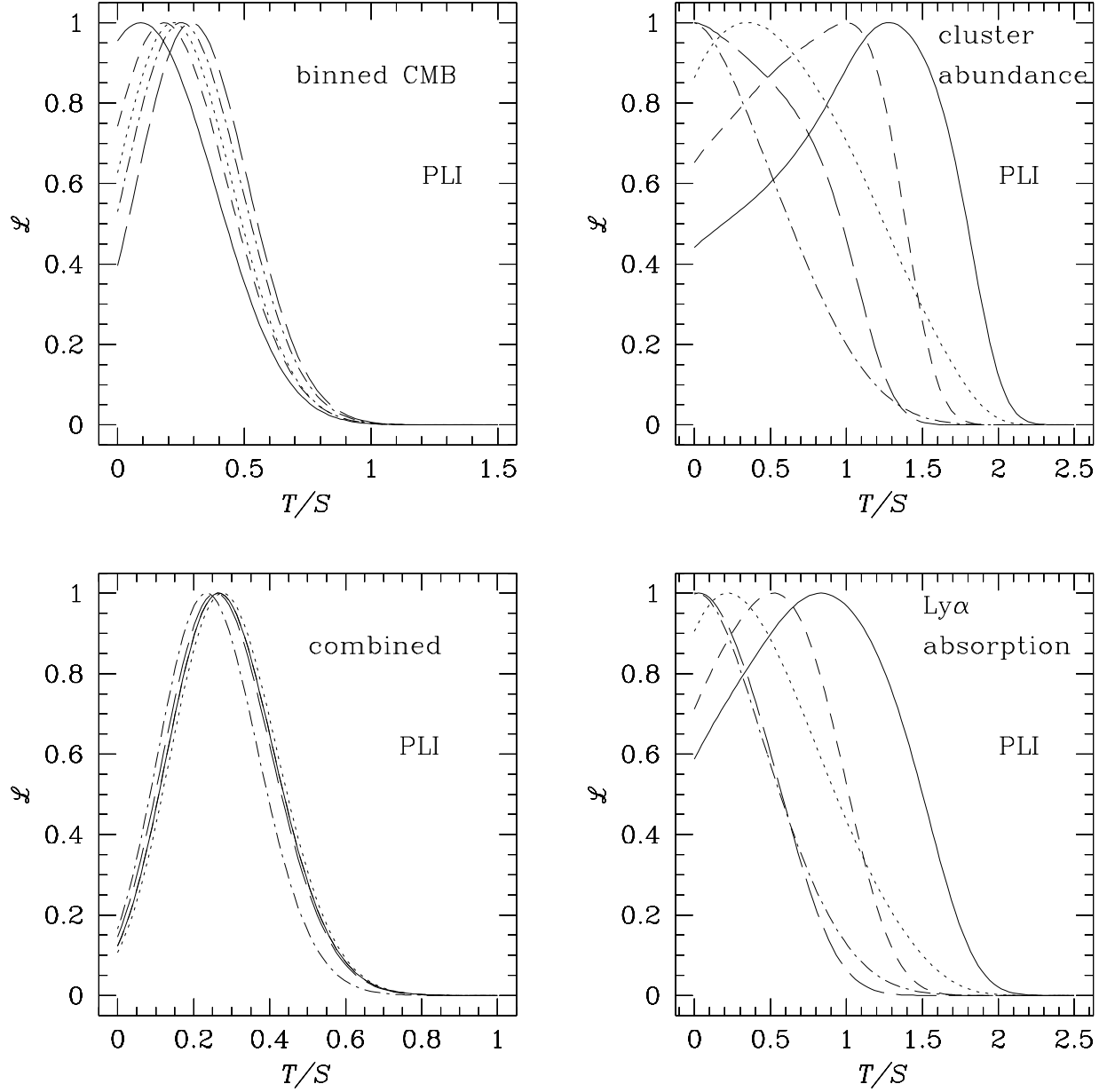


FIG. 3. Integrated likelihoods versus T/S for PLI and for the various data sets; clockwise from upper left: binned CMB, cluster abundance, $\text{Ly}\alpha$ absorption, and combined data. Solid, short-dashed, long-dashed, dotted, and dot-dashed curves represent no constraint, $t_0 > 11$ Gyr, $t_0 > 13$ Gyr, cluster baryon fraction, and SNe Ia parameter constraints, respectively.

TABLE I. 95% confidence limits on T/S for various data sets and parameter constraints, and for power-law inflation. “2.5+” represents no constraint (for values as high as this we do not expect our approximations to be adequate in any case).

Data set	No constraint	$t_0 > 11$ Gyr	$t_0 > 13$ Gyr	Cluster baryon	Supernova
<i>COBE</i>	2.1	2.1	2.1	2.1	2.1
binned CMB	0.60	0.62	0.67	0.63	0.65
galaxy correlations	2.5+	2.5+	2.5+	2.5+	2.5+
cluster abundance	1.8	1.4	1.1	1.5	1.1
Ly α absorption	1.6	1.1	0.82	1.3	0.96
combined	0.52	0.52	0.51	0.53	0.47

TABLE II. 95% confidence limits for T/S as for Table I but for ϕ^p inflation.

Data set	No constraint	$t_0 > 11$ Gyr	$t_0 > 13$ Gyr	Cluster baryon	Supernova
binned CMB	0.63	0.64	0.67	0.64	0.65
galaxy correlations	2.5+	2.5+	2.5+	2.5+	2.5+
cluster abundance	2.1	1.5	1.2	1.8	1.2
Ly α absorption	1.8	1.2	0.87	1.5	1.1
combined	0.49	0.49	0.49	0.50	0.45

decreases the power at small scales, improving the fit over Λ CDM, and thus reducing the need for tensors. When an age constraint is applied, we force the model towards lower h and Ω_0 according to Eq. (28), and hence towards lower T/S , as is seen in Fig. 3. The cluster baryon and supernova constraints similarly move us to smaller Ω_0 .

Figure 4 displays likelihoods versus p for ϕ^p inflation, while Fig. 5 presents likelihoods versus T/S for the case of free tensor contribution and $n_s = 1$. In all plots, curves have been omitted for the very weakly constraining data sets. The curves of Fig. 4 closely resemble those of Fig. 3. This is because, for $p \gg 2$, Eqs. (5), (6), and (7) give $T/S \simeq -6.85 \tilde{n}$, which is similar to the PLI result of Eq. (3).

In Fig. 5 we see that the data are considerably less constraining, compared with the PLI case, when we allow T/S to vary freely. This was expected, since in the PLI case, the lowering of n_s tends to enhance the effect of increasing T/S . We also expect that a blue scalar tilt would oppose the effect of tensors on the spectrum and hence allow larger T/S . Figure 6 illustrates this effect by plotting the 95% upper confidence limits on T/S versus scalar index with T/S free. Note that we cannot meaningfully constrain T/S here by marginalizing over n_s , since the best fits to the spectrum remain good even for very blue tilts and very large T/S .

Our confidence limits are summarized in Table I for the case of power-law inflation, Table II for polynomial potentials, and Table III for free T/S and $n_s = 1$. In all cases 95% upper limits on T/S are presented, after integrating over the ranges of parameter space specified in Sec. III. The row gives the data set used, while the column specifies the type of parameter constraint applied, if any.

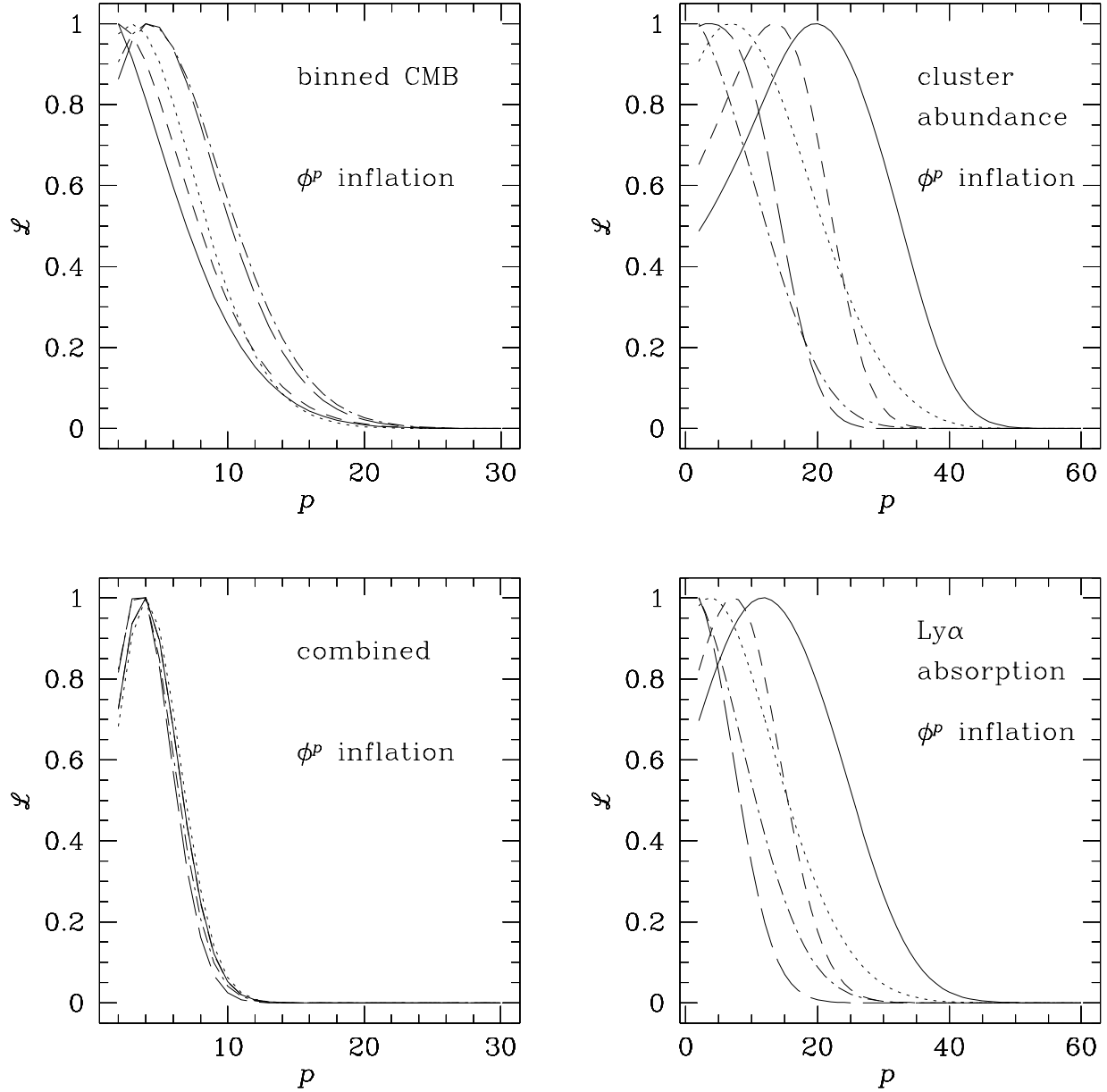


FIG. 4. Integrated likelihoods versus p for ϕ^p inflation and for various data sets; clockwise from upper left: binned CMB, cluster abundance, Ly α absorption, and combined data. Solid, short-dashed, long-dashed, dotted, and dot-dashed curves represent no constraint, $t_0 > 11$ Gyr, $t_0 > 13$ Gyr, cluster baryon fraction, and SNe Ia parameter constraints, respectively.

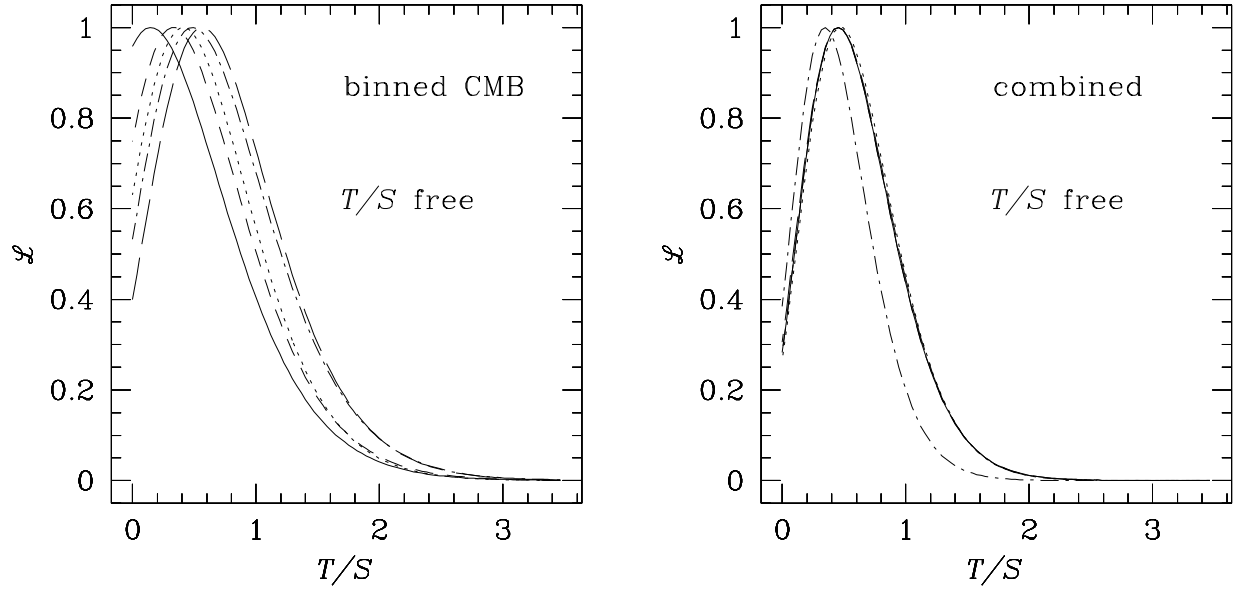


FIG. 5. Integrated likelihoods versus T/S for T/S free and $n_s = 1$, for binned CMB (left) and combined data (right). Solid, short-dashed, long-dashed, dotted, and dot-dashed curves represent no constraint, $t_0 > 11$ Gyr, $t_0 > 13$ Gyr, cluster baryon fraction, and SNe Ia parameter constraints, respectively.

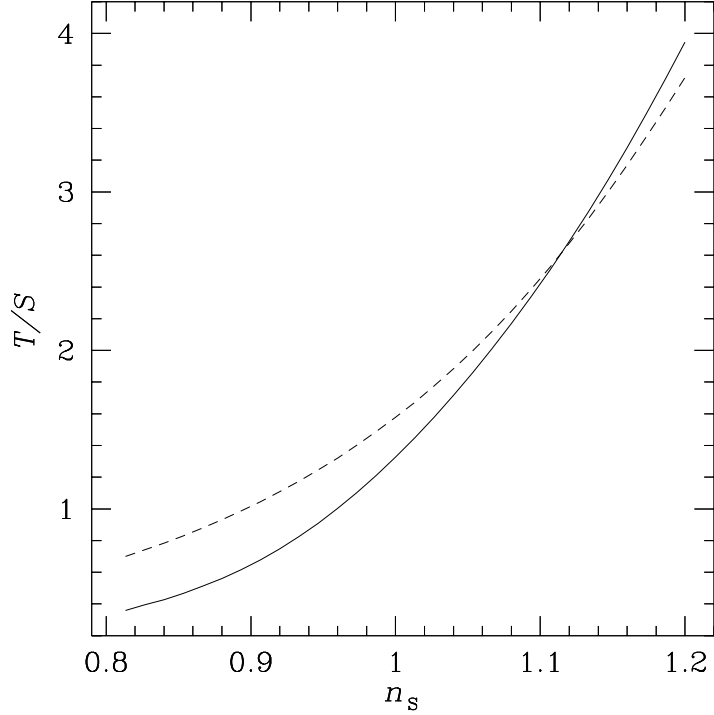


FIG. 6. 95% confidence limits on T/S versus n_s , for T/S free and for binned CMB (dashed) and combined data (solid). No parameter constraints have been applied.

TABLE III. 95% confidence limits on T/S as for Table I but for $n_s = 1$ and T/S free.

Data set	No constraint	$t_0 > 11$ Gyr	$t_0 > 13$ Gyr	Cluster baryon	Supernova
<i>COBE</i>	2.5+	2.5+	2.5+	2.5+	2.5+
binned CMB	1.6	1.6	1.8	1.6	1.8
cluster abundance	2.5+	2.5+	2.5+	2.5+	2.5+
Ly α absorption	2.5+	2.5+	2.5+	2.5+	2.5+
combined	1.3	1.3	1.3	1.3	1.0

VIII. THE FUTURE

The discovery of a nearly scale-invariant spectrum of long wavelength gravity waves would be tremendously illuminating. Inflation is the only known mechanism for producing an almost scale-invariant spectrum of adiabatic scalar fluctuations, a prediction which is slowly gaining observational support. In the simplest, “toy”, models of inflation a potentially large amplitude almost scale-invariant spectrum of gravity waves is also predicted. For monomial inflation models within the slow-roll approximation, detailed characterization of this spectrum could in principle allow a reconstruction of the inflaton potential [11]. This surely is a window onto physics at higher energies than have ever been probed before.

Inflation models based on particle physics, rather than “toy” potentials, predict a very small tensor spectrum [23]. However, essentially nothing is known about particle physics above the electroweak scale, and extrapolations of our current ideas to arbitrarily high energies could easily miss the mark. We must be guided then by observations. We have argued that observational support for a large gravity wave component is weak. Indeed observations definitely require the tensor anisotropy to be subdominant for large angle CMB anisotropies. On the other hand, it is still possible to have $T/S \simeq 0.5$, and since it would be so exciting to discover any tensor signal at all we are led to ask: how small can a tensor component be and still be detectable? What are the best ways to look for a tensor signal?

A. Direct detection

The feasibility of the direct detection of inflation-produced gravitational waves has been addressed by a number of authors [2,53–58], with pessimism expressed by most.

The ground-based laser interferometers LIGO and VIRGO [59] will operate in the $f \sim 100$ Hz frequency band, while the European Space Agency’s proposed space-based interferometer LISA [60] would operate in the $f \sim 10^{-4}$ Hz band. Millisecond pulsar timing is sensitive to waves with periods on the order of the observation time, *i.e.* frequencies $f \sim 10^{-7} - 10^{-9}$ Hz [59]. These instruments probe regions of the tensor perturbation spectrum which entered during the radiation dominated era. Expressions for the fraction of the critical density due to gravity waves per logarithmic frequency interval can be found in [53–57]. Assuming that $\Omega_0 = 1$ in a PLI model, with the only relativistic particles being photons and 3 neutrino species, and taking the *COBE* quadrupole $Q = T + S \simeq 4.4 \times 10^{-11}$, one finds [57]

$$\Omega_{\text{GW}}(f)h^2 = 5.1 \times 10^{-15} \frac{n_{\text{T}}}{n_{\text{T}} - 1/7} \exp \left[n_{\text{T}} N + \frac{1}{2} N^2 (dn_{\text{T}}/d \ln k) \right], \quad (33)$$

where $N \equiv \ln(k/H_0)$ and $n_{\text{T}} = -(T/S)/7$ is the tensor spectral index.

Using Eq. (33) Turner [57] found that the local energy density in gravity waves is maximized at $T/S = 0.18$ for $f \sim 10^{-4}$ Hz. At this maximum, the local energy density is in the range $\Omega_{\text{GW}}h^2 \simeq 10^{-15} - 10^{-16}$, which lies a couple of orders of magnitude below the expected sensitivity of LISA, and several orders below that of LIGO/VIRGO [59]. This is also well below the current upper limit of $\Omega_{\text{GW}}h^2 < 6 \times 10^{-8}$ (at 95% confidence) from pulsar

timing [61]. As T/S increases above 0.18, $\Omega_{\text{GW}}(f \sim 10^{-4}\text{Hz})h^2$ begins to *decrease* due to the increasing magnitude of the tensor spectral index.

Recall that our joint data constraint for PLI gives $T/S \lesssim 0.5$, so our results predict that the inflationary spectrum of gravity waves from PLI is not amenable to direct detection.

B. Limits from the CMB

With the advent of *MAP* and especially the *Planck* Surveyor, with its higher sensitivity, detailed maps of the CMB are just around the corner. What do we expect will be possible from these missions? This question has been dealt with extensively before. Assuming a cosmic variance limited experiment capable of determining only the anisotropy in the CMB but with all other parameters known, one can measure T/S only if it is larger than about 10% [62]. A more realistic assessment for *MAP* and *Planck* suggests this limit is rarely reached in practice [63,64].

However the ability to measure linear polarization in the CMB anisotropy offers the prospect of improving the sensitivity to tensor modes (for a recent review of polarization see [65]). In addition to the temperature anisotropy, two components of the linear polarization can be measured. It is convenient to split the polarization into parity even (*E*-mode) and parity odd (*B*-mode) combinations – named after the familiar parity transformation properties of the electric and magnetic fields, but not to be confused with the *E* and *B* fields of the electromagnetic radiation.

Polarization offers two advantages over the temperature. First, with more observables the error bars on parameters are tightened. In addition the polarization breaks the degeneracy between reionization and a tensor component, allowing extraction of smaller levels of signal [66]. Model dependent constraints on a tensor mode as low as 1% appear to be possible with the *Planck* satellite [63,64,67,68]. Extensive observations of patches of the sky from the ground (or satellites even further into the future) could in principle push the sensitivity even deeper.

There is a further handle on the tensor signal however. Since scalar modes have no “handedness” they generate only parity even, or *E*-mode polarization [66,69]. A definitive detection of *B*-mode polarization would thus indicate the presence of other modes, with tensors being more likely since vector modes decay cosmologically. Moreover a comparison of the *B*-mode, *E*-mode and temperature signals can definitively distinguish tensors from other sources of perturbation (*e.g.* [70]).

Unfortunately the detection of a *B*-mode polarization will prove a formidable experimental challenge. The level of the signal, shown in Fig. 7 for $T/S = 0.01, 0.1$ and 1.0 , is very small. As an indicative number, with $T/S = 0.5$, our upper limit, the *total* rms *B*-mode signal, integrated over ℓ , is $0.24 \mu\text{K}$ in a critical density universe. These sensitivity requirements, coupled with our current poor state of knowledge of the relevant polarized foregrounds make it seem unlikely a *B*-mode signal will be detected in the near future.

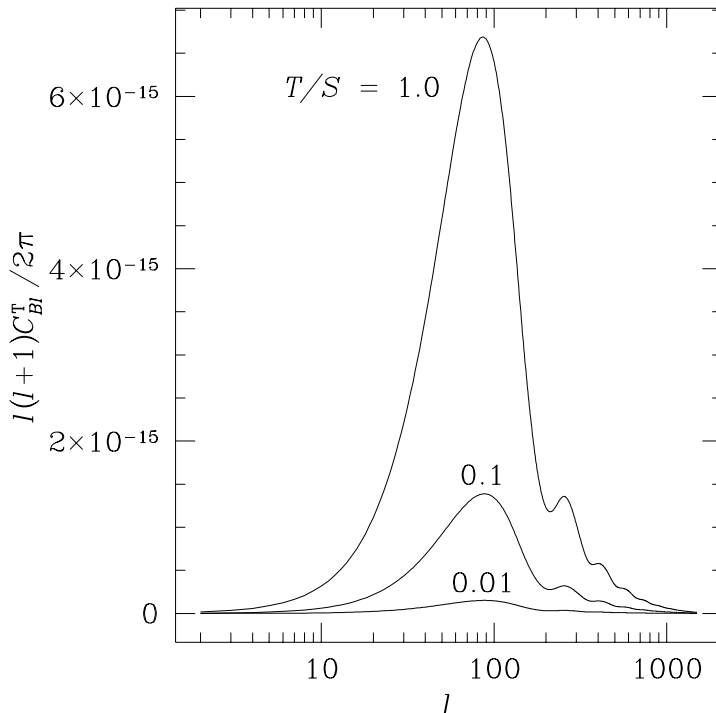


FIG. 7. B -mode tensor polarization signal $C_{B\ell}^T$ for $T/S = 0.01, 0.1,$ and 1.0 , with the remaining parameters specified as standard CDM.

IX. CONCLUSIONS

We have examined the current experimental limits on the tensor-to-scalar ratio. Using the *COBE* results, as well as small-scale CMB observations, and measurements of galaxy correlations, cluster abundances, and Ly α absorption we have obtained conservative limits on the tensor fraction for some specific inflationary models. Importantly, we have considered models with a wide range of cosmological parameters, rather than fixing the values of Ω_0 , H_0 , etc. For power-law inflation, for example, we find that $T/S < 0.52$ at the 95% confidence level. Similar constraints apply to ϕ^p inflaton models, corresponding to approximately $p < 8$. Much of this constraint on the tensor-to-scalar ratio comes from the relation between T/S and the scalar spectral index n_s in these theories. For models with tensor amplitude unrelated to *scalar* spectral index it is still possible to have $T/S > 1$. Currently the tightest constraint is provided by the combined CMB data sets. Since the quality of such data are expected to improve dramatically in the near future, we expect much tighter constraints (or more interestingly a real detection) in the coming years.

ACKNOWLEDGMENTS

This research was supported by the Natural Sciences and Engineering Research Council of Canada. M.W. is supported by the NSF.

REFERENCES

- [1] A. A. Starobinskii, *Soviet Astr. Lett.* **11**, 133 (1985).
- [2] L. M. Krauss and M. White, *Phys. Rev. Lett.* **69**, 869 (1992).
- [3] R. L. Davis *et al.*, *Phys. Rev. Lett.* **69**, 1856 (1992) [erratum **70**, 1733].
- [4] D. H. Lyth and A. R. Liddle, *Phys. Lett. B* **291**, 391 (1992).
- [5] T. Souradeep and V. Sahni, *Mod. Phys. Lett.* **A7**, 3541 (1992).
- [6] D. S. Salopek, *Phys. Rev. Lett.* **69**, 3602 (1992).
- [7] A. V. Markevich and A. A. Starobinsky, *Astron. Lett.* **22**, 431 (1996).
- [8] M. Tegmark, *Astrophys. J.* **514**, L69 (1999).
- [9] J. Lesgourgues, D. Polarski, and A. A. Starobinsky, astro-ph/9807019.
- [10] A. Melchiorri, M. V. Sazhin, V. V. Shulga, and N. Vittorio, astro-ph/9901220.
- [11] A. R. Liddle and D. H. Lyth, *Phys. Rep.* **231**, 1 (1993); J. E. Lidsey, *et al.*, *Rev. Mod. Phys.* **69**, 373 (1997); D. H. Lyth and A. Riotto, *Phys. Rep.* **314**, 1 (1999).
- [12] M. S. Turner and M. White, *Phys. Rev. D* **53**, 6822 (1996).
- [13] K. Coble, S. Dodelson, and J. A. Frieman, *Phys. Rev. D* **55**, 1851 (1997).
- [14] R. R. Caldwell and P. J. Steinhardt, *Phys. Rev. D* **57**, 6057 (1998).
- [15] A. D. Linde, *Phys. Lett. B* **129**, 177 (1983); A. D. Linde, *Particle Physics and Inflationary Cosmology* (Harwood Academic, Chur, Switzerland, 1990).
- [16] A. A. Starobinsky and J. Yokoyama, gr-qc/9502002; J. García-Bellido and D. Wands, *Phys. Rev. D* **52**, 6739 (1995); M. Sasaki and E. D. Stewart, *Prog. Theor. Phys.* **95**, 71 (1996); J. García-Bellido and D. Wands, *Phys. Rev. D* **53**, 5437 (1996); T. T. Nakamura and E. D. Stewart, *Phys. Lett. B* **381**, 413 (1996).
- [17] A. D. Linde, *Phys. Lett. B* **259**, 38 (1991); A. D. Linde, *Phys. Rev. D* **49**, 748 (1994); E. J. Copeland, A. R. Liddle, D. H. Lyth, E. D. Stewart, and D. Wands, *Phys. Rev. D* **49**, 6410 (1994).
- [18] A. R. Liddle, in *From Quantum Fluctuations to Cosmological Structures: Proceedings of the First Moroccan School of Astrophysics*, edited by D. Valls-Gabaud *et al.*, *Astronomical Society of the Pacific Conference Series* **126**, 31 (1997).
- [19] D. La and P. J. Steinhardt, *Phys. Rev. Lett.* **62**, 376 (1989).
- [20] E. W. Kolb, *Physica Scripta* **T36**, 199 (1991).
- [21] B. Whitt, *Phys. Lett. B* **145**, 176 (1984); K. Maeda, *Phys. Rev. D* **39**, 3159 (1989); D. Wands, *Class. Quant. Grav.* **11**, 269 (1994).
- [22] S. Dodelson, W. H. Kinney, and E. W. Kolb, *Phys. Rev. D* **56**, 3207 (1997).
- [23] D. H. Lyth, *Phys. Rev. Lett.* **78**, 1861 (1997); D. H. Lyth and A. Riotto, *Phys. Rep.* **314**, 1 (1999).
- [24] L. F. Abbott and M. B. Wise, *Nucl. Phys.* **B244**, 541 (1984).
- [25] F. Lucchin and S. Matarrese, *Phys. Rev. D* **32**, 1316 (1985).
- [26] A. Linde, *Phys. Lett. B* **129**, 177 (1983).
- [27] G. F. Smoot and D. Scott in the Review of Particle Properties, C. Caso *et al.*, *The European Physical Journal* **C3**, 127 (1998).
- [28] J. R. Bond, A. H. Jaffe, and L. E. Knox, *Phys. Rev. D* **57**, 2117 (1998).
- [29] J. R. Bond, A. H. Jaffe, and L. E. Knox, astro-ph/9808264.
- [30] M. White, *Phys. Rev. D* **53**, 3011 (1996).
- [31] U. Seljak and M. Zaldarriaga, *Astrophys. J.* **469**, 437 (1996).

- [32] E. F. Bunn and M. White, *Astrophys. J.* **480**, 6 (1997).
- [33] J. M. Bardeen, J. R. Bond, N. Kaiser, and A. S. Szalay, *Astrophys. J.* **304**, 15 (1986).
- [34] N. Sugiyama, *Astrophys. J. Supp.* **100**, 281 (1995).
- [35] J. A. Peacock and S. J. Dodds, *Mon. Not. R. Astron. Soc.* **267**, 1020 (1994).
- [36] R. J. Scherrer and D. H. Weinberg, *Astrophys. J.* **504**, 607 (1998).
- [37] J. A. Peacock, *Mon. Not. R. Astron. Soc.* **284**, 885 (1997).
- [38] P. T. P. Viana and A. R. Liddle, *Mon. Not. R. Astron. Soc.* **303**, 535 (1999).
- [39] A. R. Liddle, D. H. Lyth, P. T. P. Viana, and M. White, *Mon. Not. R. Astron. Soc.* **282**, 281 (1996).
- [40] E. F. Bunn, A. R. Liddle, and M. White, *Phys. Rev. D* **54**, 5917 (1996).
- [41] R. A. C. Croft, D. H. Weinberg, M. Pettini, L. Hernquist, and N. Katz, *astro-ph/9809401*.
- [42] S. M. Carroll, W. H. Press, and E. L. Turner, *Annu. Rev. Astron. Astrophys.* **30**, 499 (1992).
- [43] D. A. Vandenberg, P. B. Stetson, and M. Bolte, *Annu. Rev. Astron. Astrophys.* **34**, 461 (1996).
- [44] B. Chaboyer, *Phys. Rep.* **307**, 23 (1998).
- [45] D. A. White and A. Fabian, *Mon. Not. R. Astron. Soc.* **273**, 72 (1995).
- [46] A. V. Filippenko and A. G. Riess, *Phys. Rep.* **307**, 31 (1998).
- [47] J. R. Gott, *Nature* **295**, 304 (1982); M. Sasaki, T. Tanaka, K. Yamamoto, and J. Yokoyama, *Phys. Lett. B* **317**, 510 (1993); M. Bucher, A. S. Goldhaber, and N. Turok, *Phys. Rev. D* **52**, 3314 (1995); A. D. Linde and A. Mezhlumian, *Phys. Rev. D* **52**, 6789 (1995).
- [48] M. Tanaka and M. Sasaki, *Prog. Theor. Phys.* **97**, 243 (1997).
- [49] M. Bucher and J. D. Cohn, *Phys. Rev. D.* **55**, 7461 (1997).
- [50] M. White and J. Silk, *Phys. Rev. Lett.* **77**, 4704 (1996) [erratum **78**, 3799].
- [51] M. White and D. Scott, *Comments Astrophys.* **18**, 289 (1996).
- [52] W. Hu and M. White, *Astrophys. J.* **486**, L1 (1997).
- [53] M. White, *Phys. Rev. D* **46**, 4198 (1992).
- [54] M. S. Turner, M. White, and J. E. Lidsey, *Phys. Rev. D* **48**, 4613 (1993).
- [55] M. S. Turner and M. White, *Phys. Rev. D* **53**, 6822 (1996).
- [56] A. R. Liddle, *Phys. Rev. D* **49**, 3805 (1994).
- [57] M. S. Turner, *Phys. Rev. D* **55**, R435 (1997).
- [58] R. R. Caldwell, M. Kamionkowski, and L. Wadley, *Phys. Rev. D* **59**, 027101 (1999).
- [59] K. S. Thorne, in *Particle and Nuclear Astrophysics and Cosmology in the Next Millennium, Snowmass 94*, edited by E. W. Kolb and R. D. Peccei (World Scientific, Singapore, 1995), p. 398.
- [60] K. Danzmann, *Ann. N. Y. Acad. Sci.* **759**, 481 (1995).
- [61] V. M. Kaspi, J. H. Taylor, and M. F. Ryba, *Astrophys. J.* **428**, 713 (1994).
- [62] L. Knox and M. S. Turner, *Phys. Rev. Lett.* **73**, 3347 (1994); L. Knox, *Phys. Rev. D* **52**, 4307 (1995).
- [63] M. Zaldarriaga, D. N. Spergel, and U. Seljak, *Astrophys. J.* **488**, 1 (1997).
- [64] J. R. Bond, G. Efstathiou, and M. Tegmark, *Mon. Not. R. Astron. Soc.* **291**, L33 (1997).
- [65] W. Hu and M. White, *New Astron.* **2**, 323 (1997).
- [66] M. Zaldarriaga and U. Seljak, *Phys. Rev. D* **55**, 1830 (1997); M. Zaldarriaga and U.

- Seljak, Phys. Rev. D **58**, 023003 (1998).
- [67] M. Kamionkowski and A. Kosowsky, Phys. Rev. D **57**, 685 (1998).
- [68] W. H. Kinney, Phys. Rev. D **58**, 123506 (1998).
- [69] M. Kamionkowski, A. Kosowsky, and A. Stebbins, Phys. Rev. D **55**, 7368 (1997).
- [70] W. Hu and M. White, Phys. Rev. D **56**, 596 (1997).